

Electronegativity Is the Average One-Electron Energy of the Valence-Shell Electrons in Ground-State Free Atoms

Leland C. Allen

Contribution from the Department of Chemistry, Princeton University, Princeton, New Jersey 08544-1009. Received February 27, 1989

Abstract: It is argued that electronegativity is the third dimension of the Periodic Table, and that $\chi_{\text{spec}} = (m\epsilon_p + n\epsilon_s)/(m + n)$, for representative elements where ϵ_p , ϵ_s are the p, s ionization energies and m , n the number of p, s electrons. Values of spectroscopic χ are obtained to high accuracy from the National Bureau of Standards atomic energy level tables and closely match the widely accepted Pauling and Allred & Rochow scales. χ_{spec} rationalizes the diagonal separation between metals and non-metals in the Periodic Table, the formation of noble gas molecules, metallization of the elements as one descends groups I-V, and the force definition used by Allred & Rochow. $\Delta\chi_{\text{spec}} = \chi_{\text{spec}}^A - \chi_{\text{spec}}^B$, the energy difference of an average electron in atom A and in atom B, is able to systematize properties of the vast array of known materials: ionic solids, covalent molecules, metals, minerals, inorganic and organic polymers, semiconductors, etc. Transition-metal electronegativity cannot be simply determined because of the nature of d-orbital radial distributions and this is reflected in its paucity of use among transition-metal chemists. Estimates for first transition series χ_{spec} are obtained and a computational method to address this problem is given. It also proves possible to translate free atom, ground-state χ_{spec} into the in situ molecular orbital definition of average one-electron energy for orbitals localized on an atomic center. This leads to an improved definition of group (or substituent) electronegativity, extension and refinements in the use of electronegativity perturbations in qualitative and semiquantitative molecular orbital theory, and understanding of hybrid orbital electronegativity ordering rules such as $sp^2 > sp^3$.

I. Electronegativity: Connection to Periodic Table and Properties

It is the hypothesis of this paper that electronegativity is an intimate property of the Periodic Table and that its definition follows from this relationship. The continuing and overarching chemical organizing ability of the Periodic Table strongly suggests that an additional variable, beyond the change in Z across a row and the change in shell number down a column, must play a key role in the characterization of solid-state and molecular binding. It is most likely that this new third dimension is an energy because the Schrödinger equation itself identifies energy as the central parameter for describing the structure of matter. Since the Periodic Table is comprised of rows in which a subshell increases its occupancy in one-electron steps until completion at a noble gas atom, and since successive rows simply add subshells, the new property must be the energy of a subshell. From the Aufbau Principle, we know (for the representative elements) that subshells are specified by the number of s and p electrons and thus it follows that electronegativity is defined on a per-electron (or average one-electron energy) basis as

$$\chi_{\text{spec}} = \frac{m\epsilon_p + n\epsilon_s}{m + n}$$

where m and n are the number of p and s valence electrons, respectively. The corresponding one-electron energies, ϵ_p and ϵ_s , are the multiplet-averaged total energy differences between a ground-state neutral and a singly ionized atom, and the atomic energy level data required to determine them is available at high accuracy from the National Bureau of Standard Tables.¹ χ_{spec} is termed "spectroscopic electronegativity" and a three-dimensional

Table I. Electronegativities for Representative Elements (Pauling Units)

atom	χ_{spec}^a	χ_P^b	$\chi_{A\&R}^c$	$\chi_{B\&E}^d$	χ_M^e
H	2.300	2.20	2.20		3.059
Li	0.912	0.98	0.97		1.282
Be	1.576	1.57	1.47		1.987
B	2.051	2.04	2.01	1.90	1.828
C	2.544	2.55	2.50	2.60	2.671
N	3.066	3.04	3.07	3.08	3.083
O	3.610	3.44	3.50	3.62	3.215
F	4.193	3.98	4.10	4.00	4.438
Ne	4.787				4.597
Na	0.869	0.93	1.01		1.212
Mg	1.293	1.31	1.23		1.630
Al	1.613	1.61	1.47	1.58	1.373
Si	1.916	1.90	1.74	1.87	2.033
P	2.253	2.19	2.06	2.17	2.394
S	2.589	2.58	2.44	2.64	2.651
Cl	2.869	3.16	2.83	3.05	3.535
Ar	3.242				3.359
K	0.734	0.82	0.91		1.032
Ca	1.034	1.00	1.04		1.303
Ga	1.756	1.81	1.82	1.75	1.343
Ge	1.994	2.01	2.02	1.99	1.949
As	2.211	2.18	2.20	2.21	2.256
Se	2.424	2.55	2.48	2.46	2.509
Br	2.685	2.96	2.74	2.75	3.236
Kr	2.966				2.984
Rb	0.706	0.82	0.89		0.994
Sr	0.963	0.95	0.99		1.214
In	1.656	1.78	1.49		1.298
Sn	1.824	1.96	1.72		1.833
Sb	1.984	2.05	1.82		2.061
Te	2.158	2.10	2.01		2.341
I	2.359	2.66	2.21		2.880
Xe	2.582				2.586

(1) Moore, C. E. *Atomic Energy Levels*, National Bureau of Standards Circular 467, Vol. I (1949), II (1952), III (1958) (reprinted as NSRDS-NBS 35, Vol. I, II, III). Supplements on selected second-row elements plus Si, NSRDS-NBS 3, Sections 1-11 (1965-1985). Na, Mg, Al, Si, and P: Martin, W. C., et al. *J. Phys. Chem. Ref. Data* 1979, 8, 817; 1980, 9, 1; 1981, 10, 153; 1983, 12, 323; 1985, 14, 751. Pettersson, J. E. *Phys. Scr.* 1983, 28, 421 (multiplets of (3s)(3p)⁴ for S II). Li, H.; Andrew, K. L. *J. Opt. Soc. Am.* 1971, 61, 96; 1972, 62, 255 (multiplets of (4s)(4p)³ for As II). Arcimowicz, B.; Aufmuth, P. *J. Opt. Soc. Am.* 1987, 4B, 1291 (⁴S₂ multiplet of (5s)(5p)³ for Sb II). *Bibliography on the Analysis of Optical Atomic Spectra*, NBS Special Publications 306 (1968), 306-2 (1969), 306-3 (1969), 306-4 (1969). *Bibliography on Atomic Energy Levels and Spectra*, NBS Special Publications 363, 1968-1971, 1971-1975, 1975-1979, 1979-1983. Also valuable for updates: Radzig, A. A.; Smirnov, B. M. *Reference Data on Atoms, Molecules, and Ions*; Springer-Verlag: New York, 1985; Springer Series in Chemical Physics, Vol. 31.

^a The scale factor set by χ_{spec} average of Ge and As = the combined average of the Allred and Rochow and Pauling values for Ge and As. Thus absolute values in Rydbergs were multiplied by 2.30016. ^b Pauling, data from ref 6. ^c Allred and Rochow, ref 7. ^d Boyd and Edgcombe, values taken directly from Table I of ref 8. ^e Mulliken, data from ref 30. Same scale factor convention as used for χ_{spec} ; thus absolute values in kJ were multiplied by 0.004419.

map for the representative elements through the 5th row is given as Figure 1. The numbers from the NBS tables give absolute values in Rydbergs and a single scale factor (set near the center

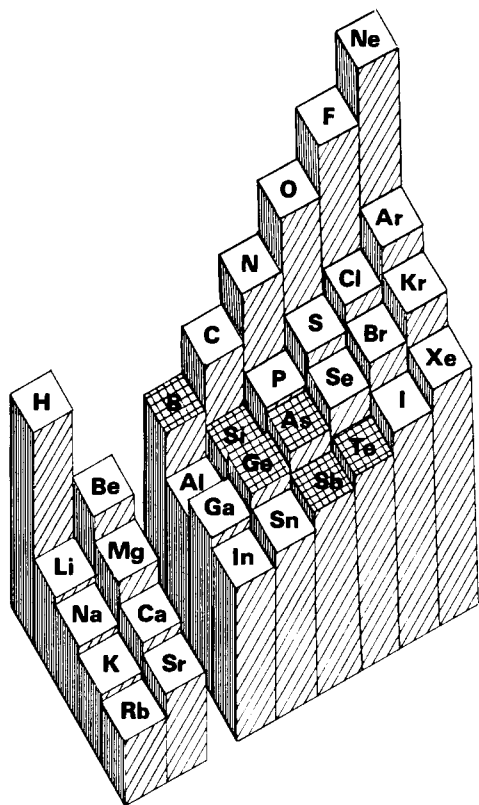


Figure 1. Electronegativity, $\chi_{\text{spec}} = (m\epsilon_p + n\epsilon_s)/(m + n)$, where m , ϵ_p , n , ϵ_s are the number and ionization potentials (multiplet averaged) of p and s electrons in the valence shell of representative elements through the 5th row. ϵ_p and ϵ_s were obtained from National Bureau of Standards high-resolution atomic energy level tables (ref 1). Cross-hatched atoms are those of the metalloid band.

of the metalloid band) converts them to the Pauling scale. It is to be noted especially that both χ_{spec} and the Periodic Table are defined by free atoms in their ground states.

χ_{spec} versus Rows. If we plot χ_{spec} versus row number (Figure 2 and Table I) we may expect a set of nearly parallel curves that fall off rather rapidly with increasing row number. This result follows because atoms are nearly spherical and each left-to-right isoelectronic step is of increasing subshell radius, therefore decreasing energy. Each vertical step downward from one curve to another removes one electron therefore yielding successive decreases in average valence shell energy as one moves from top to bottom in Figure 2. The upward shift at the fourth row for p-block elements (and consequent alternation in groups III and IV) is a result of incomplete s, p valence shell screening by 3d electrons as one passes through the first transition series. (The screening primarily affects the s electrons because of their non-zero charge density at the nucleus. The incomplete d screening affects the fifth row as well as the fourth.) The metalloid band is also designated in Figure 2 and it is apparent that this region encompasses just those atoms, and only those atoms, known to be metalloids.² This band is appropriately narrow since it represents the most important diagonal relationship in the Periodic Table, that which separates the non-metals from the metals. The diagonal nature of this dividing band implies that it is a consequence of the Periodic Table's third dimension. We show below that there is a fixed relationship between χ_{spec} , free atom energy level spacings, and energy band widths in solids, thereby establishing the connection between χ_{spec} and the physical basis for differentiating metallic solids and liquids from non-metals.

Noble Gas Atom χ_{spec} . The noble gas atoms are logically the top curve in Figure 2 and χ_{spec} characterizes the known chemistry of these elements. Thus, e.g. Ne (Figure 2) has a higher χ_{spec} than any open-shell atom and therefore holds its electrons too tightly

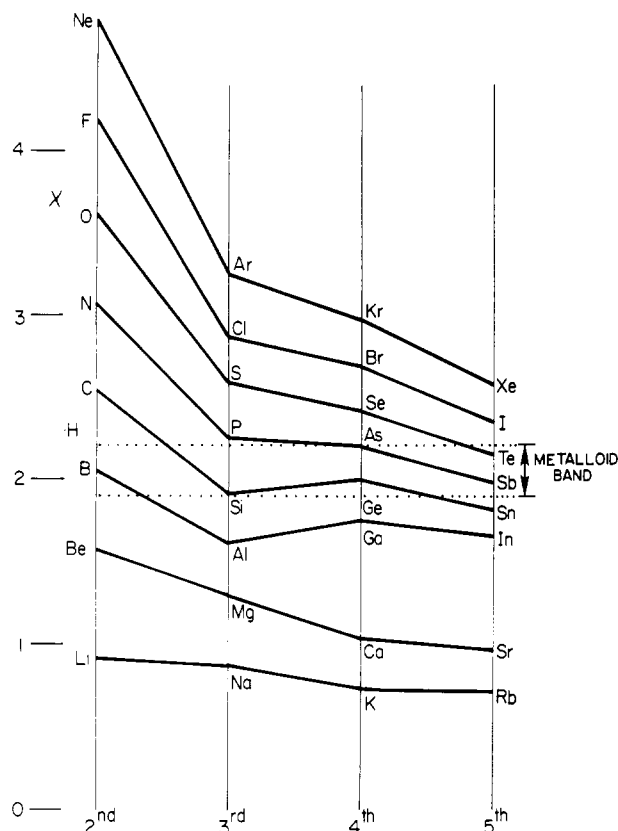


Figure 2. χ_{spec} from experimental atomic energy level data versus rows. Family of curves for groups I–VIII of the representative elements. Pauling units (scale set by equating χ_{spec} average of Ge and As to combined average of Allred & Rochow and Pauling scale Ge and As values). Metalloid band has Si as the lower limit and As as the upper limit.

to permit chemical bonding. On the other hand, the difference in χ_{spec} values between Xe and F or O easily rationalizes the known oxides and fluorides of Xe, and the relatively large $\Delta\chi_{\text{spec}}$ between Kr and F accounts for the existence of KrF_2 . But $\Delta\chi_{\text{spec}}$ between Xe and Cl and between Xe and N are sufficiently smaller to suggest that no binary molecules free of a stabilizing environment (produced, e.g., by crystallization) are likely to be found.^{3a} We are still left with the tantalizing question of whether ArF_2 can be realized ($\Delta\chi_{\text{spec}}$ across ArF is only 8% smaller than across XeO) and with the outside possibility of a krypton oxide. Noble gas atoms form the hinge of the Periodic Table because their electronegativity is two-sided: they have the values shown for their role of *holding* electrons, but all have a χ_{spec} of zero for *attracting* electrons.^{3b}

Comparison with Pauling and Allred & Rochow Scales. Pauling's electronegativity scale was first published in 1932⁴ and many others have been proposed since then. However, an extensive search of the literature (textbooks, journal articles, and review papers⁵) show that values from only two, Pauling's scale (as up-dated by Allred in 1961)⁶ and those from Allred & Rochow's force definition,⁷ have been frequently and systematically employed by chemists and physicists to guide them in answering practical problems in chemical bonding. Figure 3 compares values from these two with χ_{spec} , and it is immediately apparent that χ_{spec} is reproducing the pattern established by the Pauling and Allred & Rochow scales. In fact, χ_{spec} seems to adjudicate them. It may be that χ_{spec} for F, and perhaps O, are 1–2% too high, this possibility arising from their extremely high density thereby producing

(3) (a) XeCl_2 is obtainable in a xenon matrix but is too unstable to be chemically characterized. The non-binary compounds, $\text{Xe}(\text{CF}_3)_2$ and $\text{FXeN}(\text{SO}_2\text{F})_2$, have strong electron-withdrawing groups attached to C or N. (b) Allen, L. C.; Huheey, J. E. *J. Inorg. Nucl. Chem.* **1980**, *42*, 1523.

(4) Pauling, L. *J. Am. Chem. Soc.* **1932**, *54*, 3570.

(5) Allen, L. C., to be submitted to *Chem. Rev.*

(6) Allred, A. L. *J. Inorg. Nucl. Chem.* **1961**, *17*, 215.

(7) Allred, A. L.; Rochow, E. G. *J. Inorg. Nucl. Chem.* **1958**, *5*, 264.

(2) Rochow, E. G. *The Metalloids*; D. C. Heath & Co., 1966.

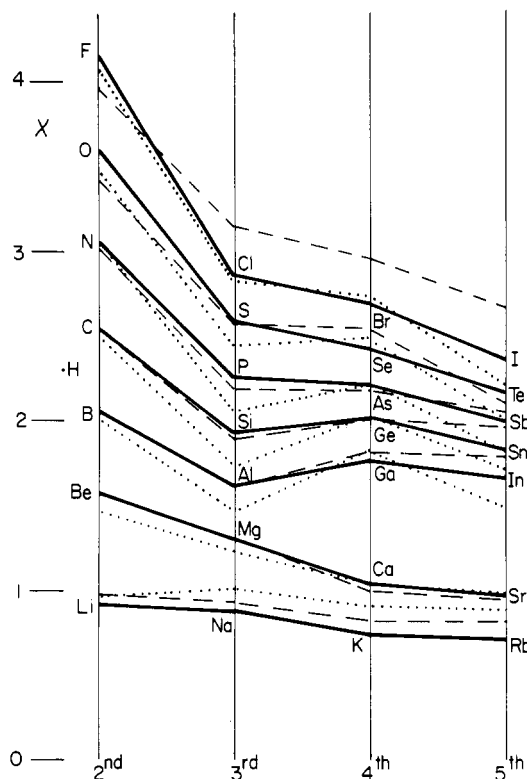


Figure 3. χ_{spec} , experimental values (solid lines), compared to Pauling scale (dashed lines) and to Allred & Rochow scale (dotted lines).

differentially high electron-electron correlation energy corrections when they bind to form molecules or solids. Similarly, group I χ_{spec} may be 5–6% too low because of the differentially high charge transfer binding that may be expected when they bond into solids or molecules.

The Allred & Rochow force definition,⁷ $\chi_A = 0.359Z_A/r_A^2 + 0.744$, where Z_A is the Slater rule determined effective nuclear charge and r_A is the Pauling covalent radius, has appealed conceptually to many chemists. It is thus satisfying that a set of linear relationships exist between χ_{spec} and the force on the outermost electrons at their radial maxima (shown in part VI below).

Comparison with Boyd & Edgecombe's Scale. Very recently, Boyd and Edgecombe⁸ have determined electronegativities from computed electron density distributions for a number of representative element hydrides, XH. Atomic radii were determined by the point of minimum charge density along X–H and electronegativity was assumed to be a direct function of the charge density at the minimum, the number of valence electrons, and the X–H separation and an inverse function of the atomic radii. This appears to be a plausible and promising approach and comparison between their values and χ_{spec} for p-block elements is given in Figure 4 (and Table I⁹). The Boyd–Edgecombe definition is very different from that of either Allred & Rochow or Pauling and thus the striking agreement obtained in Figure 4 is encouraging.

$\Delta\chi_{\text{spec}}$ and Ketelaar's Triangle. Pauling's well-known procedure for equating the bond energy above that expected from a perfect sharing distribution to a function of $\chi_A - \chi_B$ (designated as the ionic character of $AB^{10,11}$) has a clear conceptual relationship to

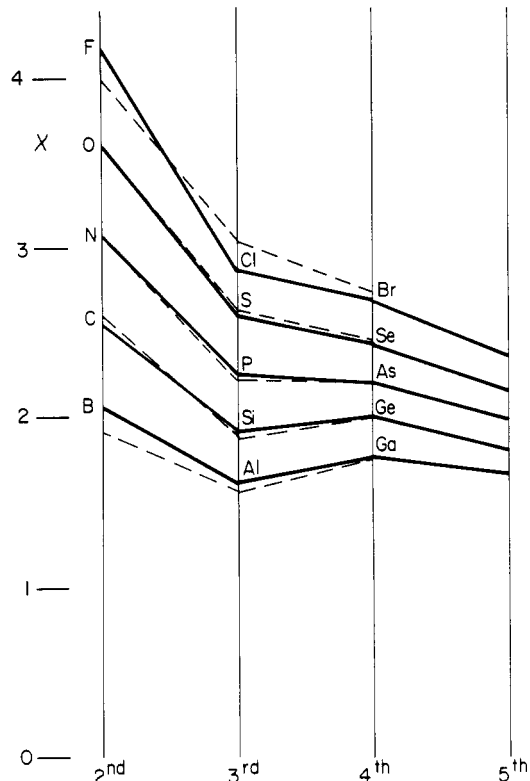


Figure 4. χ_{spec} , experimental values (solid lines), compared to 15 p-block elements from Boyd & Edgecombe values (dashed lines) computed from electron density distributions.

$\chi_{\text{spec}}^A - \chi_{\text{spec}}^B$. Thus we identify $\chi_{\text{spec}}^A - \chi_{\text{spec}}^B \equiv \Delta\chi_{\text{spec}}$ as the ionic character or *bond polarity* of bond AB. $\Delta\chi_{\text{spec}}$ and the Periodic Table of χ_{spec} govern the three types of bonds¹² (covalent, metallic, and ionic) traditionally employed¹³ to characterize the chemical and physical properties of materials in the temperature and pressure range where metals and ionic compounds occur as solids and liquids.¹⁴ This is demonstrated most easily by visualizing Ketelaar's triangle¹⁵ whose vertices are labeled covalent, metallic, and ionic. Covalent and metallic bonds have long been recognized as originating from the same basic quantum mechanical maximum overlap-exchange forces¹⁶ and therefore along this side of the triangle we are simply moving right to left in the Periodic Table. For the elements themselves, the change from diatomics (F_2 , O_2 , N_2) to metals (Li, Na) is ruled by χ_{spec} (see the description of the non-metal/metal transition given in part III below). For heteroatomic bonds, e.g., HF compared to H_2 and F_2 , it is readily apparent that $\Delta\chi_{\text{spec}}$ determines bond polarity. Thus, χ_{spec}^H and χ_{spec}^F are the average energies of the one-electron atomic orbitals needed to construct the usual molecular orbital energy level diagram commonly employed to explain the bonding in HF. The difference in these average one-electron energies measures the shift in molecular charge distribution giving rise to the HF bond polarity.

(12) The fourth type of bonding, London dispersion forces and molecular multipole interactions, characterizes the cohesion in molecular liquids and solids, including inert gas liquids and solids. The magnitudes of many such interactions are also governed by $\Delta\chi_{\text{spec}}$, but the Periodic Table plays a less direct role in organizing them than it does for the other three.

(13) Spice, J. E. *Chemical Binding and Structure*; Pergamon Press: New York, 1964. Seel, F. *Atomic Structure and Chemical Bonding*; Methuen: London, 1963. Ketelaar, J. A. A. *Chemical Constitution*; Elsevier: New York, 1958. Companion, A. L. *Chemical Bonding*; McGraw-Hill: New York, 1964. Pimental, G. C.; Spratley, R. D. *Chemical Bonding Clarified Through Quantum Mechanics*; Holden-Day: San Francisco, 1969.

(14) At high temperatures, of course, matter is solely in the form of atoms and covalently bound molecules.

(15) Ketelaar, J. A. A. *Chemical Constitution*; Elsevier: New York, 1958; Chapter I.

(16) Slater, J. C. *Introduction to Chemical Physics*; McGraw-Hill: New York, 1939; Chapter 22.

(8) Boyd, R. J.; Edgecombe, K. E. *J. Am. Chem. Soc.* **1988**, *110*, 4182.
(9) Problems with this definition for the six low-electronegativity elements of groups I and II, seemingly from charge-transfer effects, leads to values very far from those of Allred & Rochow and Pauling.

(10) Pauling, L. *The Nature of the Chemical Bond*, 3rd ed.; Cornell University Press, 1960; Chapter 3.

(11) In the original construction of his scale⁴ and in further research summarized in *The Nature of the Chemical Bond*,¹⁰ Pauling has directed his quantitative efforts toward establishing electronegativity values for free atoms. However, in his qualitative introductory paragraph, he associates electronegativity with "the power of an atom in a molecule to attract electrons to itself". We identify "... in a molecule ..." with the all embracing molecular properties ordering capability of the Periodic Table.

Table II. Structural Classification of Ionic-Covalent Compounds

A. Classification of Representative Element Fluorides in Their Group Oxidation States							
I	II	III	IV	V	VI	VII	
LiF	BeF ₂	BF ₃	CF ₄				
NaF	MgF ₂	AlF ₃	SiF ₄	PF ₅	SF ₆		
KF	CaF ₂	GaF ₃	GeF ₄	AsF ₅	SeF ₆		
RbF	SrF ₂	InF ₃	SnF ₄	SbF ₅	TeF ₆	IF ₇	
ionic		polymeric			molecular covalent		
B. A List of Simple Oxides of the Representative Elements							
I	II	III	IV	V	VI	VII	VIII
Li ₂ O	BeO	B ₂ O ₃	CO ₂	NO, N ₂ O, N ₂ O ₃	O ₂	FO ₂ , O ₄ F ₂	
Na ₂ O	MgO	Al ₂ O ₃	CO	N ₂ O ₄ , N ₂ O ₅		F ₂ O ₂	
			SiO ₂	P ₄ O ₆ , P ₄ O ₁₀	SO ₂ , SO ₃	Cl ₂ O, ClO ₂	
K ₂ O	CaO	Ga ₂ O ₃	GeO ₂	As ₂ O ₃ , As ₄ O ₆	SeO ₂ , SeO ₃	Cl ₂ O ₇	
Rb ₂ O	SrO	In ₂ O ₃	SnO ₂	Sb ₂ O ₃ , Sb ₄ O ₆	TeO ₂ , TeO ₃	Br ₂ O, BrO ₂	
			SnO	Sb ₂ O ₅		I ₂ O ₄ , I ₄ O ₉	XeO ₃
						I ₂ O ₅	XeO ₄
C. Structural Classification of Representative Element Oxides							
I	II	III	IV	V	VI	VII	VIII
Li	Be	B	C	N	O	F	
Na	Mg	Al	Si	P	S	Cl	
K	Ca	Ga	Ge	As	Se	Br	
Rb	Sr	In	Sn	Sb	Te	I	
							Xe
ionic		polymeric			molecular covalent		

An important subcategory along the covalent-metallic side is the semiconductors. These are the covalent solids of metalloid band elements (e.g., Si, Ge) or binary compounds with a metalloid (e.g., GaAs, InSb, SiC) or binaries straddling this band (e.g., AlP, GaP). As discussed previously, the metalloid band is defined by a specific range of χ_{spec} values and thus χ_{spec} and $\Delta\chi_{\text{spec}}$ classify the bonding in these materials.

Along the ionic-covalent leg of Ketelaar's triangle decreasing $\Delta\chi_{\text{spec}}$ determines the properties of typical binary compounds as illustrated by the species shown in Table II.^{17,18} On the left side of Table IIA are the representative element fluorides that adopt classic ionic structures (e.g., LiF, MgF₂) and on the right a collection of ten well-known covalently bound individual molecules. Between these limits is the interesting diagonal-shaped region, delineated quite accurately by $\Delta\chi_{\text{spec}}$, the structure of whose compounds are polymeric solids (e.g., in AlF₃, GaF₃, and InF₃ the metals are coordinated octahedrally with shared vertices; BeF₂ has a silica-like structure). Table IIB lists simple oxides of the representative elements and Table IIC classifies them structurally. Again we find well-recognized ionic compounds on the left (e.g., MgO, sodium chloride structure; Na₂O, antifluorite; Al₂O₃, corundum and its closely related C-M₂O₃ ionic structure for Ga₂O₃ and In₂O₃ both of which have approximately octahedral coordination around M³⁺ and approximately tetrahedral around O²⁻, and SnO₂ with an ionic 6:3 rutile structure) and on the right discrete covalently bound molecules (e.g., CO₂, SO₂, NO, O₄F₂, FO₂, XeO₃). In between are polymeric materials, (e.g., B₂O₃, a 3-connected, silicate-like network; SiO₂ and GeO₂ the α -quartz structure; P₄O₆ and P₄O₁₀, metastable molecules transformable into two-dimensional or three-dimensional networks that are also formed by the arsenic and antimony oxides; SeO₂, 3-connected infinite chains; TeO₂ layer and three-dimensional networks). Tables IIA and IIC with their diagonal-shaped polymeric regions

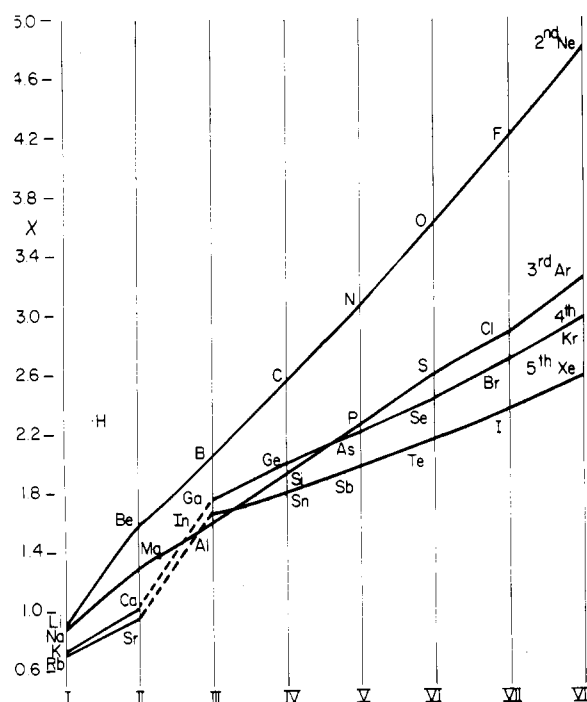


Figure 5. χ_{spec} , experimental values, versus groups for the first five rows of representative elements. Pauling units. Values are given in Table I.

defined by χ_{spec} are typical of a large amount of data that can be classified in this fashion.¹⁷ Similarly, along the metallic-to-ionic side $\Delta\chi_{\text{spec}}$ characterizes the sequential change from pure metals to ionic crystals (e.g., Li, Li₃Sb, Li₃As, Li₃P, Li₃N, Li₂O, LiF: Li₃Sb has the intermetallic Fe₃Al structure derived from cubic close packing; Li₃As has complex alloy-like phases; Li₃P forms as well as Li₃P and the lithium phosphorus bond is intermediate, neither metallic or ionic, while Li₃N, Li₂O, and LiF are ionic species progressing to the extreme).

χ_{spec} versus Groups. Figure 5 plots χ_{spec} versus group number and the pattern of interrelationships displayed is surprisingly different from that of Figure 2, even though the data are the same in both maps. For each row, χ_{spec} is rising nearly linearly with Z, but the incomplete d-screening in the transition series, dif-

(17) Puddephatt, R. J.; Monaghan, P. K. *The Periodic Table of the Elements*, 2nd ed.; Clarendon Press: Oxford, 1986. Wells, A. F. *Structural Inorganic Chemistry*, 4th ed.; Clarendon Press: Oxford, 1975.

(18) An excellent quantum mechanical discussion of the relationship between ionic and covalent bonding is given in: Slater, J. C. *Quantum Theory of Molecules and Solids, Volume 2, Symmetry and Energy Bands in Crystals*; McGraw-Hill: 1965; Chapter 4. *J. Chem. Phys.* **1964**, *41*, 3199. Slater's analysis provides the basis for the ability of $\Delta\chi_{\text{spec}}$ to characterize the change in bond polarity as bonding changes from ionic to covalent, thus playing a role for the ionic-covalent leg of Ketelaar's triangle similar to that which his work cited in ref 16 provided for the metal-covalent leg (see part III).

ferences in screening between s and p electrons, and the successively lower slopes due to increasing radii lead to an intricately ordered set of values for groups III–V of the 3rd, 4th, and 5th rows. This forcefully brings out the requirement for the high-accuracy values provided by χ_{spec} and speaks against the impression of many chemists that only order-of-magnitude electronegativity estimates are needed. Contemporary research on semiconductor–electrolyte and semiconductor–metal junctions is one example of solid-state physics and chemistry where accurate electronegativity values for groups III–VI of the 3rd, 4th, and 5th rows will prove useful.¹⁹ For some time the magnitude of 5th row electronegativities has been in dispute and this is readily apparent in their differing magnitudes on the Pauling and Allred & Rochow scales (Table I). Another long-standing uncertainty has been the value for Cl relative to N, many chemists favoring the Pauling scale assignment of chlorine greater than nitrogen. Table I shows that the reverse is true and the difference is comparable to that between Ge and As or Cl and Br. One consequence of the lower electronegativity of Cl compared to N is the structural dissimilarity between FN_3 and ClN_3 .²⁰

As we descend any of the group I, II, III, IV, or V lines in Figure 5, χ_{spec} decreases and characterizes the increasing metallization.²¹ The s, p, and d levels are getting closer together and there is a corresponding loss of bond directionality. Group IV is a classical example: starting with diamond, the tetrahedrally coordinated, covalently bonded, insulator (or with the highly directional bonding in graphite layers), the next three elements, Si, Ge, gray Sn, are tetrahedrally coordinated semiconductors with successively decreasing energy gaps. The final two are metals with increasing conductivities: white Sn, distorted from tetrahedral coordination by compression along the c axis giving it approximately six nearest neighbors and Pb, face-centered cubic with 12 nearest neighbors.

H bonds, $\text{A}\cdots\text{H}\cdots\text{B}$, are another well-known form of bonding whose dominant characterizing parameter is electronegativity difference, $\Delta\chi = \chi_{\text{A}} - \chi_{\text{H}}$.²² Less well-known, but equally important, are Alcock's secondary bonds,²³ a type of non-hydrogen, hydrogen bond, $\text{A}\cdots\text{Y}\cdots\text{B}$. For example,²³ the solid $\text{ClF}_2^+\text{SbF}_6^-$ contains a linear bonding arrangement, $\text{F}\cdots\text{Cl}\cdots\text{F}$, where $r(\text{F}\cdots\text{Cl}) = 1.52 \text{ \AA}$ and $r(\text{Cl}\cdots\text{F}) = 2.38 \text{ \AA}$. As in hydrogen bonds, $\text{A}\cdots\text{Y}\cdots\text{B}$ is typically linear, B has an electron donor lone pair, and $r(\text{Y}\cdots\text{B})$ is significantly larger than $r(\text{A}\cdots\text{Y})$ but shorter than the sum of van der Waals radii. A great variety of such bonds are found in inorganic solids and $\Delta\chi_{\text{spec}} = \chi_{\text{spec}}^{\text{A}} - \chi_{\text{spec}}^{\text{Y}}$ controls $r(\text{Y}\cdots\text{B})$, bond strength, and other properties, as it does in the case of hydrogen bonds.²⁴ In summary, the description of bonding patterns in this and the previous section suggests that χ_{spec} , because it can be determined accurately and is the third dimension of the Periodic Table, may replace many specialized and ad hoc explanations of solid-state and molecular properties, thereby fulfilling the role of Occam's razor.

Transition-Metal Electronegativity. An important conclusion is that transition element electronegativities cannot be simply determined due to the nature of d-orbital radial distributions. This is not surprising: the literature of transition-metal chemistry routinely employs antibonding d-orbital occupancy, oxidation state, and formal charge on ligands as characterizing parameters but electronegativity is rarely mentioned. In the representative elements the radii of the outermost s and p electrons are approximately the same while in the transition elements the s orbital radii are $2^{1/2}$ to $3^{1/2}$ times greater than the d orbital radii. Nevertheless, it is well-known that d-electrons contribute significantly to the bonding orbitals in both pure metals and complexes with non-

metals but their degree of participation is difficult to assign. The number of participating d-electrons decreases across a row because the ratio of the outer s radial maxima to the d radial maxima becomes significantly larger and because the d orbital energy sharply decreases (becomes more core-like). As described in the section below, we have devised a quantum mechanical computational method to quantify the bonding contribution and the effective number of d-electrons for particular molecules and solids, but we can also make an approximate estimate for the first transition series by using well-known information from inorganic chemistry. Thus we use our χ_{spec} formula for s- and d-electrons plus the following assumptions. (i) Because χ_{spec} is the third dimension of the Periodic Table, the highest value for a transition element must be equal to or less than the lowest value in the metalloid band (Si, 1.916). (ii) The first half of the d-block is treated like the first half of the p-block because the observed maximum oxidation states²⁵ suggest that all of the s- and d-electrons can fully participate in chemical bonding. However, except for Ru and Os, the elements in the second half do not realize maximum oxidation states equal to the number of outer s- and d-electrons in the free atoms²⁵ (this is a result of the decrease in the number of effective d-electrons caused by the reasons given above). For the first transition series we interpret the sequential maximum oxidation state decrease in Fe, Co, and Ni by one for each step to the right²⁵ as successive loss of one d-electron and assume this pattern for Cu and Zn. (iii) The 4s orbital is assumed doubly occupied because the 4s is widely split on molecule formation and the bonding MOs dominated by this orbital will always be doubly occupied. (iv) The one-electron energies used in the χ_{spec} equation are taken from Herman & Skillman (see part V below for references and comparison with experiment). χ_{spec} values (reference to Au(V) = 1.90 to satisfy (i)) are the following: Sc, 1.15; Ti, 1.28; V, 1.42; Cr, 1.57; Mn, 1.74; Fe, 1.79; Co, 1.82; Ni, 1.80; Cu, 1.74; Zn, 1.60 (if the recently observed Cu(IV) is used instead of Cu(III), it raises $\chi_{\text{spec}}^{\text{Cu}}$ by a few percent). These values closely parallel the experimental numbers from the Pauling scale definition obtained by Allred⁶ (with the single exception of Mn whose low-value Allred attributes to a crystal field stabilization effect). The trends in χ_{spec} are those expected from the traditional transition element groupings in the Periodic Table: a smooth rise with Z, like that of the representative elements, for Sc through Mn; quite similar, high values for Fe, Co, and Ni; Cu by itself and slightly lower than the Fe, Co, Ni triad; Zn very much lower with a value close to that of Al.²⁶

In Situ Electronegativity. We have emphasized throughout this paper that electronegativity is a free-atom, ground-state quantity and that it derives its meaning as an extension of the Periodic Table. By the same argument, the Periodic Table itself achieves its miraculous ability to organize chemical phenomena to a considerable extent because χ_{spec} is its third dimension. Thus, the Periodic Table and χ_{spec} together comprise the small set of rules and numbers that help rationalize the observed properties of the 10 million known compounds, but they stand apart from the vastly complicated bonding details represented in these many molecules and solids. Therefore, an in situ electronegativity defined for a

(19) Sculfort, J.-L.; Gautron, J. *J. Chem. Phys.* **1984**, *80*, 3767 and reference therein.

(20) Allen, L. C.; Peters, N. J. S., in preparation.

(21) Adams, D. M. *Inorganic Solids*; John Wiley & Co.: New York, 1974.

(22) Allen, L. C. *J. Am. Chem. Soc.* **1975**, *97*, 6921; *Proc. Natl. Acad. Sci. U.S.A.* **1975**, *72*, 4701.

(23) Alcock, N. W. *Adv. Inorg. Radiochem.* **1972**, *15*, 2.

(24) Desmeules, P. J.; Nuchtern, J.; Allen, L. C., to be published.

(25) Huheey, J. E. *Inorganic Chemistry*, 3rd ed.; Harper & Row: New York, 1983; 569–572. Purcell, K. F.; Kotz, J. C. *Inorganic Chemistry*; W. B. Sanders, 1977; pp 530–531.

(26) Because χ_{spec} is a free atom quantity with a single defining number for each element, it cannot depend on oxidation state. While it is certainly true that atoms have different electronegativities for different oxidation states, e.g. F_3CH versus CH_4 (this can be readily measured by the difference in hydrogen bond energy realized between $\text{F}_3\text{C}\cdots\text{H}$ and $\text{H}_3\text{C}\cdots\text{H}$ as proton donor), search of the literature⁹ shows that representative element chemists generally have not found a need for assuming a strong dependence. Representative elements of groups I and II have such low χ_{spec} that they are always in their group number oxidation state. Polar covalent bonds formed by p-block elements carry atomic charges that are seldom close to their oxidation number therefore suggesting small changes in electronegativity with change in molecular environment. On the other hand, the closely spaced levels found in transition metal containing molecules and solids has given rise to the belief that transition metal electronegativity should be strongly dependent on oxidation state. As in the case of main group elements, some dependence is certainly to be expected, but at present the strength of this dependence is unknown.

solid or molecule can only produce numbers of very specific interest for the particular compounds studied and not the generality of the free-atom values.²⁶ We also recall that, as Pauling pointed out in his original paper,⁴ it is the *difference* in electronegativity across a bond *AB* that is of prime importance and that this difference is to be a measure of *ionic character* of *AB* and to not include its covalent component. In spite of these considerations, it is a useful and straightforward task to set up a projection operator and apply it to a molecular orbital wave function to yield in situ average one-electron energies for atoms in molecules. The difference of these numbers for atoms A and B, when appropriately referenced to homonuclear bonds AA and BB, is then the desired in situ electronegativity difference and we have designated it the *Bond Polarity Index*, BPI_{AB} . (The mathematical formulae are given in part VII below.) Within the context of free-atom χ_{spec} , the role of BPI_{AB} is 2-fold: (1) It makes connection between free-atom $\Delta\chi_{spec}$ and the detailed determination of *bond polarity* in molecules and solids from ab initio electronic wave functions as well as the incorporation of electronegativity concepts into qualitative and semiquantitative molecular orbital theory.²⁷ (2) Ab initio calculations on a wide variety of transition-metal complexes can hopefully lead to atomic electronegativities for the transition elements including their dependence on oxidation state.²⁶ A set of preliminary calculations are quite encouraging in this regard.²⁸ It is also a simple matter to define an *Fractional Polarity*²⁸ from the Bond Polarity Index and this is the equivalent of Pauling's dipole moment referenced "percent ionic character". Results from the same set of preliminary calculations are similarly supportive.

II. Other Definitions of Electronegativity

We have already noted the unique standing of the Pauling and Allred & Rochow scales as being those which χ_{spec} was obligated to match. In this section we discuss central features of the Mulliken definition because it is also unique in providing the principal conceptual alternative to χ_{spec} (even though various tabulations of values based on Mulliken concepts have not enjoyed widespread acceptance among practicing chemists and physicists). We address only those aspects that may directly challenge χ_{spec} as the energy dimension of the Periodic Table. In a soon to be completed review article,⁵ we attempt to treat the other parts of the vast and complex history of electronegativity.

The simplest form of the Mulliken²⁹ definition is given as

$$\chi_M = (I + A)/2$$

where *I* is the lowest first ionization potential of a ground-state free atom and *A* is its corresponding electron affinity. A principal attraction of this definition (as well as the second form discussed below) among theoretical chemists and physicists has been that it has the units of energy per electron. We regard this as important support also for χ_{spec} , which is expressed in the same units. Figure 6 plots χ_M versus rows for this definition with use of the latest experimental data³⁰ (referenced in the same way to a point in the metalloid band, as employed in Figure 2; values given in Table I). Comparing Figure 6 to Figures 2 and 3 shows a very rough similarity, but many incorrect features are readily apparent. The most obvious are the following: (a) The metalloid band is much too wide and contains the metals Be and Sn in addition to the

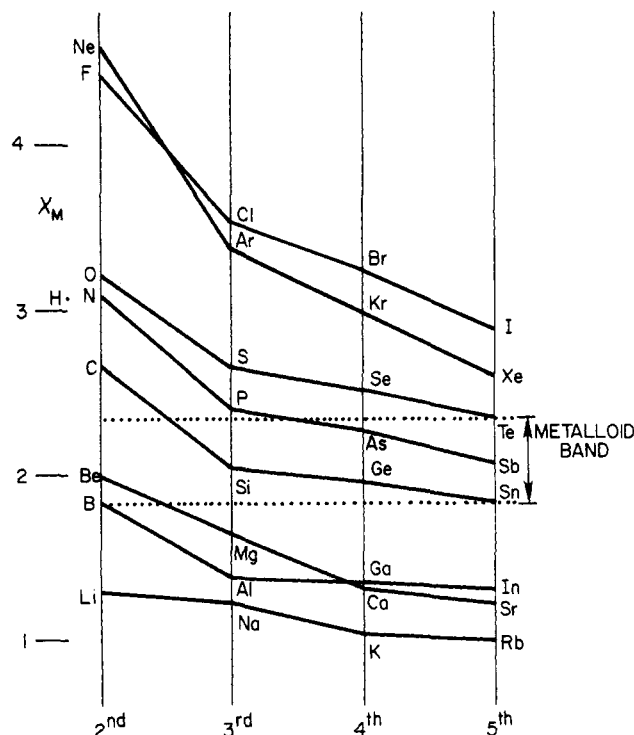


Figure 6. $\chi_M = (I + A)/2$, Mulliken definition of electronegativity, versus rows. *I* and *A* are experimental ground state first ionization potentials and electron affinities, respectively (values from ref 30). Pauling units (χ_M values and referencing given in Table I). Metalloid band set to include known metalloids (B, Si, Ge, As, Sb, Te).

metalloids. (b) Hydrogen has a higher value than carbon. (c) There is no alternation in χ_M magnitudes between 3rd and 4th row elements (Si-Ge, Al-Ga). As noted previously, alternation is due to incomplete screening of 4s electrons by the 3ds of the first transition series and it is an experimentally well-established criterion for judging electronegativity scales.^{31,32} (d) The group VII halogens are too high and cross with the noble gas atoms. (e) Groups II and III cross, with the former too high and the latter too low. The origins of these problems are largely the result of two basic flaws in the Mulliken definition. The first is lack of s electron representation. The s electrons certainly enter into representative element chemical bonding, change their relative contributions across a row, and must obviously influence bond polarity. The second is that *I* and *A* are treated symmetrically in the χ_M equation. *I* may be identified as the energy of an electron in the outer shell of a neutral atom and *A* the corresponding energy in the negative ion, but in most neutral molecules the atomic charges are much nearer to 0 than to -1.

A second form of the Mulliken definition, "valence state χ_v ", identifies a specified atomic hybridization and computes I_v and A_v from ground-state *I* and *A* plus promotion energies to the atomic excited state designated. Data from the NBS atomic energy level tables¹ are used to obtain promotion energies of the s and p electrons into excited states with orbital occupancies of 0, 1, and 2 corresponding to the desired valence state. This definition clearly avoids the problem of omitting s electrons. Bratsch has given an up-to-date account of this scheme³³ and in a recent complete tabulation of values Bergmann and Hinze³⁴ list 124 possible hybridizations and corresponding Pauling-scale electronegativities for the sulfur atom alone. This method seeks to address a specific atom in a specific molecule and the chief difficulty, of course, is that there is no a priori way to make such

(27) The Pauling concept of relating the electronegativity difference for bond *AB* to the excess energy above the mean of the AA and BB bond energies¹⁰ remains as the best basis for obtaining experimental estimates of free atom values from molecular and solid-state data. The Bond Polarity Index then forms the link between free atoms and (referenced) in situ atoms. It is obvious, of course, that the comparison between free atom $\Delta\chi$ and in situ $\Delta\chi$ can only be made on a *relative* basis because the average one-electron energy of a free atom is very different than an average one-electron atomic energy in situ due to molecular bonding energy. Controversies and practical problems with the Pauling scale are discussed in ref 5.

(28) Allen, L. C.; Egolt, D. A.; Knight, E. T.; Liang, C., to be submitted. The principal feature of EI_A and BPI_{AB} is their ability to assign a *local energy* (albeit, one-electron energy) to an atom or to the difference between bonded atoms.

(29) Mulliken, R. S. *J. Chem. Phys.* **1934**, *2*, 782.

(30) Reference 1 for ionization potentials. Hotop, H.; Lineberger, W. C. *J. Phys. Chem. Ref. Data* **1985**, *14*, 731, for electron affinities.

(31) Sanderson, R. T. *J. Am. Chem. Soc.* **1952**, *74*, 4792.

(32) Allred, A. L.; Rochow, E. G. *J. Inorg. Chem.* **1958**, *5*, 269.

(33) Bratsch, S. G. *J. Chem. Ed.*, **1988**, *65*, 34, 223.

(34) Bergmann, D.; Hinze, J. *Electronegativity and Charge Distribution. In Structure and Bonding*; Sen, K. D., Jørgensen, C. K., Eds.; Springer-Verlag: New York, 1987; Vol. 66.

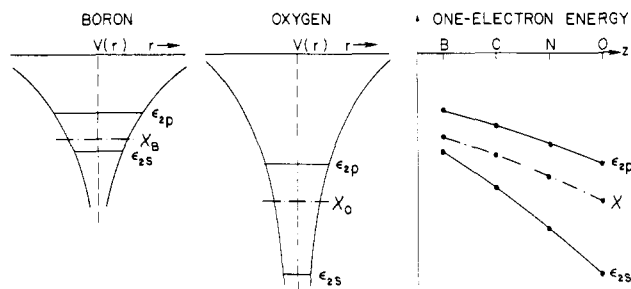


Figure 7. Left side: Schematic of effective radial potentials for boron and oxygen with energy values for ϵ_p , ϵ_s , and χ_{spec} designated. Right side: One-electron energies, ϵ_p , ϵ_s , and χ_{spec} , versus atomic number, Z , for B, C, N, and O.

valence state assignments. As Bratsch concludes,³³ "This is a very serious problem".

III. Non-Metal to Metal Transition

It is the purpose of this section to explain why a single parameter, the magnitude of χ_{spec} , is adequate to characterize the transition from non-metal to metal for the elements in the temperature and pressure range for which metals in their typical structures (face-centered cubic (fcc), body-centered cubic (bcc), hexagonal close-packed (hcp)) occur. The basis for this explanation is to be found in an elegant description of interatomic interactions given by Slater some time ago¹⁶ and by a thorough treatment of elementary electronic structure models for solids given by Waugh.³⁵ On the right, high χ , side of the Periodic Table only diatomic covalent bonds occur (N_2 , O_2 , F_2). The average energy of an electron (χ_{spec}) is very high and s and p atomic energy levels (ϵ_s , ϵ_p) are widely separated: there is no other bonding option and exchange energy locks them into homonuclear covalent bonds. As shown in Figure 7, large χ_{spec} and large energy level spacing are directly related. Like the H atom itself, the effective potential seen by an electron in an atom is funnel-shaped and this form of potential has the property that lower energy is correlated with larger spacing between levels. Thus high χ_{spec} implies widely spaced levels, both for occupied and unoccupied levels, and therefore also large HOMO-LUMO energy gaps. As we progress to the left along a given row of the Periodic Table the energy level spacing decreases as χ_{spec} decreases. Now if a given atom is surrounded by others, energy bands will appear and the width of a band is inversely proportional to the energy of the level from which it arises. Thus small χ_{spec} corresponds to small energy level spacing and broad, frequently overlapping, energy bands. Small spacing and broad bands guarantee electron deficiency along with the electrical conductivity and ductility associated with the metallic state. If high χ atoms are clustered together they will form diatomic molecules showing saturation of valence rather than metals because the barrier between coalescing atoms will be high, the levels widely separated, and the bands narrow.

IV. Experimental Determination of χ_{spec}

Because Pauling's original assignment of 4.0 for fluorine's electronegativity was arbitrary and because of the long-sustained uncertainty as to its appropriate units, it has been difficult to obtain physical and chemical insight as to what magnitude and range of values to expect. This quandary is mediated by defining electronegativity as the average valence shell ionization potential and by the experimental finding that its values extend from approximately 4 to 25 eV, just the spread of ionization potentials and energies one expects to find identified with electronic phenomena in chemistry and solid-state physics. It is also useful to recognize that on the Pauling scale a change of 1 in the first place after the decimal point corresponds to approximately 14 kcal/mol.

ϵ_p and ϵ_s . In his 1955 Physical Review paper, and more extensively in his books on atomic structure, Slater defined one-electron energies and how they are to be determined from the

SINGLE CONFIGURATION, LS COUPLED, MULTIPLY AVERAGED, ONE ELECTRON ENERGIES

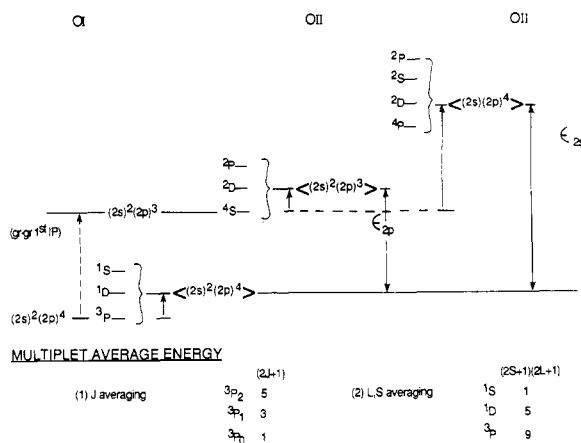


Figure 8. Schematic of the energy level diagram for neutral and singly ionized oxygen (designated O I and O II, respectively). The diagram defines single configuration $((2s)^2(2p)^4)$ multiplet averaged values for oxygen ϵ_{2p} and ϵ_{2s} . (For comparison, the dashed arrow at the left side represents the ground-state O I to ground-state O II first ionization potential usually given in elementary textbooks.)

experimental spectra of atoms and solids.³⁶ Almost all of the energy level data required to obtain valence shell ϵ_p and ϵ_s are available from the well-established high-accuracy methods of gas-phase atomic spectroscopy and largely tabulated in the publications of the U.S. National Bureau of Standards.¹ One-electron valence shell atomic energies for ground-state free atoms (e.g. ϵ_{2p} and ϵ_{2s} for oxygen) are obtained from the difference in the multiplet averages $((2L+1)(2S+1)$ average) of the neutral atom ground-state configuration (e.g. $(2s)^2(2p)^4$ O I) and the singly ionized configurations (e.g. $(2s)^2(2p)^3$ O II for ϵ_{2p} and $(2s)(2p)^4$ O II for ϵ_{2s}) as shown schematically in Figure 8 (for pedagogical clarification the first ionization potential of O usually given in textbooks is shown as the dashed arrow between $(2s)^2(2p)^4$ and $(2s)^2(2p)^3$ on the left side of Figure 8). The very small energy level separations associated with the different values of the J quantum number are averaged out with $(2J+1)$ weighting before the multiplet averaging. Except for the special cases discussed below, the calculation of ϵ_p and ϵ_s , and consequently of χ_{spec} , is straightforward, although it should be noted that the accuracy of atomic energy level data is constantly improving, e.g., the multiplet levels for $(3s)(3p)^3$ of P II have been up-graded enough in the last 4 years to reverse the electronegativities of phosphorus and arsenic. Values for ϵ_p , ϵ_s , and χ_{spec} are given in Table III and compared with the theoretically computed values discussed in part V below.

Br, Se, and Te Special Cases. For Br II one of the multiplets in each of the configurations $(4s)^2(4p)^4$ and $(4s)(4p)^5$ has not been observed. These were determined by linear extrapolation of the E_{av} values found by Hansen and Persson³⁷ for the $(4s)^2(4p)^4$ and $(4s)(4p)^5$ configurations of Kr III, Rb IV, and Sr V. E_{av} is shown in Figure 8 as the single headed arrows from the lowest multiplet $((2s)^2(2p)^3)$ $4s$ in O II to the center of gravity of the multiplets of interest $((2s)^2(2p)^3)$ for ϵ_{2p} in O II and $((2s)(2p)^4)$ for ϵ_{2s} in O II. It has usually been obtained by spectroscopists from least-squares fits of observed spectral lines in isoelectronic sequences of atoms (thus with successively higher ionization states)

(36) Slater, J. C. *Quantum Theory of Atomic Structure*; McGraw-Hill: New York, 1960; Vol. I and II. Slater, J. C. *Phys. Rev.* **1955**, *98*, 1039. In Table I of the *Phys. Rev.* article and Table 8-2, page 206 of Vol. I, Slater has given ϵ_p and ϵ_s values for H to Sr and this served as a valuable check on the numbers we report in Table III. We have extended the number of atoms included, tabulated additional significant figures, corrected three or four errors, and used the up-graded spectra available since Slater's tabulation.

(37) Hansen, J. E.; Persson, W. J. *Opt. Soc. Am.* **1974**, *64*, 696.

(38) Persson, W.; Pettersson, S.-G. *Phys. Scr.* **1984**, *29*, 308. It should be noted here that E_{av} , the spherically averaged energies from which we determine ϵ_p and ϵ_s , are independent of the coupling scheme³⁹ (LS, LK, jK, or jj).

(35) Waugh, J. L. T. *The Constitution of Inorganic Compounds*; Wiley-Interscience: New York, 1972.

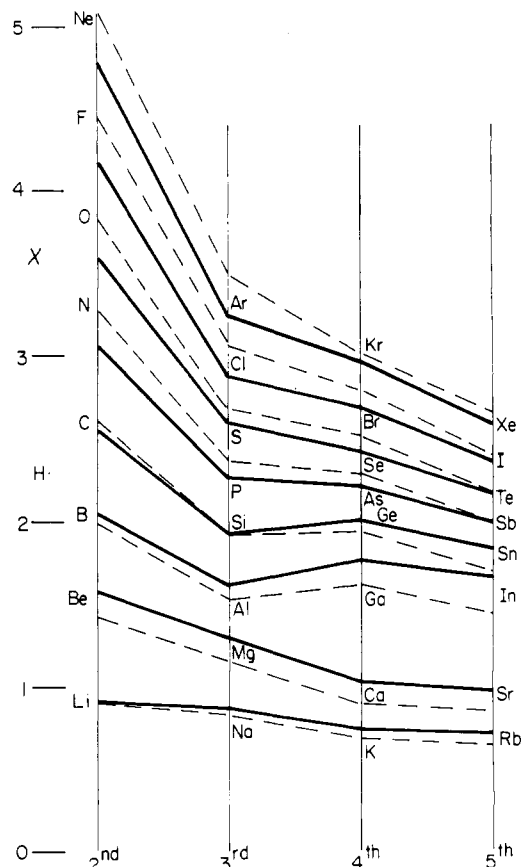
Table III. Experimental and Computed χ_{spec} Values (Rydbergs)

atom	ϵ_p^a	ϵ_s^a	exptl ^a	Hartree-Fock ^b	Hartree-Fock-Slater ^c
H		1.0000	1.0000	1.0000	
Li		0.3963	0.3963	0.3926	0.4039
Be		0.6852	0.6852	0.6186	0.6012
B	0.6098	1.0323	0.8915	0.8662	0.7792
C	0.7838	1.4282	1.1060	1.1390	0.9749
N	0.9687	1.8784	1.3326	1.4374	1.1851
O	1.1646	2.3796	1.5696	1.6722	1.4086
F	1.3709	2.9526	1.8228	1.9414	1.6458
Ne	1.5870	3.5628	2.0810	2.2408	1.8953
Na		0.3778	0.3778	0.3642	0.3777
Mg		0.5620	0.5620	0.5060	0.5051
Al	0.4393	0.8320	0.7011	0.6646	0.6157
Si	0.5716	1.0942	0.8329	0.8368	0.7389
P	0.7095	1.3848	0.9796	1.0270	0.8719
S	0.8537	1.6689	1.1254	1.1696	1.0141
Cl	1.0046	1.8542	1.2473	1.3368	1.1655
Ar	1.1627	2.1491	1.4093	1.5252	1.3257
K		0.3190	0.3190	0.2948	0.3086
Ca		0.4493	0.4493	0.3910	0.3987
Ga	0.4359	0.9270	0.7633	0.7050	0.6791
Ge	0.5544	1.1796	0.8670	0.8406	0.7627
As	0.6738	1.3921	0.9611	0.9920	0.8597
Se	0.7951	1.5710	1.0537	1.0956	0.9661
Br	0.9177	1.7914	1.1673	1.2202	1.0801
Kr	1.0453	2.0222	1.2895	1.3626	1.2003
Rb		0.3070	0.3070	0.2756	0.2905
Sr		0.4186	0.4186	0.3568	0.3682
In	0.4118	0.8738	0.7198	0.6280	0.6118
Sn	0.5155	1.0702	0.7928	0.7414	0.6781
Sb	0.6178	1.2301	0.8627	0.8670	0.7561
Te	0.7196	1.3750	0.9381	0.9468	0.8417
I	0.8215	1.5352	1.0254	1.0450	0.9328
Xe	0.9235	1.7196	1.1226	1.1580	1.0277

^a $\chi_{\text{spec}} = (m\epsilon_p + n\epsilon_s)/(m + n)$; m, n = number of p and s valence electrons, data from ref 1. ^b Data from ref 41. ^c Data from ref 44.

using the radial Coulomb and exchange integrals as fitting parameters. E_{av} values for Br II $(4s)^2(4p)^4$ and $(4s)(4p)^5$ were obtained from those of Kr III and Sr V and checked by prediction of Rb IV. The assumption of linearity is only in error by 0.05% and is close to the limits of uncertainty in Hansen and Persson's E_{av} values. There are two unobserved multiplets in $(4s)(4p)^4$ of Se II and the same extrapolation procedure was used on the E_{av} values from Persson and Pettersson³⁸ for Kr IV, Rb V, and Sr VI. For Te II $(5s)(5p)^4$ no unambiguously assigned spectra exists and thus ϵ_{5s} was extrapolated from the other 5th row one-electron energies. This was not difficult because the ϵ_{ns} versus Z curves are smooth and ϵ_{5s} closely parallels ϵ_{4s} .

Configuration Interaction Corrections. Instantaneous electron-electron correlation effects must be addressed and this problem is well treated in the book by Cowan.³⁹ We illustrate this for the $(4s)(4p)^2$ configuration of Ge II using the extended configuration interaction study of Andrew, Cowan, and Giachetti.⁴⁰ Both $(4s)^2ns$ and $(4s)^2nd$ configurations can mix with $(4s)(4p)^2$ and those investigated were the $(4s)^24d$, $(4s)^25s$, and $(4s)^25d$. Fits to the spectral lines from these configurations, using their radial interaction integrals as disposable parameters, were made and E_{av} determined. It was found that $4s^25s$ contributed negligibly and that a very accurate fit could be achieved with only the $(4s)^24d$ and $(4s)^25d$ configurations yielding $E_{\text{av}} = 69\,784\text{ cm}^{-1}$ compared to $E_{\text{av}} = 66\,866\text{ cm}^{-1}$ that we obtain directly from the NBS data without configuration interaction. Thus correlation corrections change ϵ_{4s} from 1.1530 to 1.1796 Ry and $\chi_{\text{spec}}^{\text{Ge}}$ from 0.8537 to 0.8670 Ry, a 1.5% increase. Because of the close analogy between the spectra in the 4th and 5th rows we have computed

**Figure 9.** χ_{spec} , experimental values (solid lines), compared to Hartree-Fock χ_{spec} (dashed lines). Data from ref 41.

the corresponding correlation correction for Sn II $(5s)(5p)^2$ based on the E_{av} ratios found for Ge. Andrew, Cowan, and Giachetti⁴⁰ chose to study the Ge II $(4s)(4p)^2$ case because of its rather large deviation from LS coupling and the expected strong configuration mixing. In surveying configuration interaction studies in the literature we found none with greater deviations than the Ge case, therefore we have not made further correlation corrections for the entries in Table III and believe them to be within the 1.5% error range found for Ge. In addition to the analysis of experimental spectra given here, direct quantum-mechanical calculations of the atomic wave functions can also be employed to obtain ϵ_p and ϵ_s and, as described below, these provide a close check on the values listed in Table III.

V. Computational Determination of χ_{spec}

The most obvious and straightforward way to obtain ϵ_p and ϵ_s values is from canonical Hartree-Fock solutions. Results from the Clementi & Roetti Hartree-Fock tabulations⁴¹ are given as Figure 9 (and Table III). Because of Koopmans' theorem⁴² and the immediate interpretability of the Hartree-Fock equations, one very much hopes that using these ϵ_p and ϵ_s in our formula will yield values close to experimental χ_{spec} . Fortunately, Figure 9 does show that all of the significant features of the pattern are preserved, but there remains a considerable spreading out of the computed values that is undesirable. It arises from two sources: (1) the Clementi & Roetti wave functions are determined for ground-state multiplets and therefore no multiplet averaging has been carried out, and (2) correlation corrections.

A second approach attempts to eliminate both of these sources of error but still retain the simplicity of interpretation and ease of computation embodied in the canonical Hartree-Fock method. Figure 10 (and Table III) gives the results of using ϵ_p and ϵ_s values in our formula that were calculated by the Hartree-Fock-Slater

(39) Cowan, R. D. *Theory of Atomic Structure and Spectra*; University of California Press, 1981.

(40) Andrew, K. L.; Cowan, R. D.; Giachetti, A. *J. Opt. Soc. Am.* **1967**, *57*, 715.

(41) Clementi, E.; Roetti, C. *Atomic Data and Nuclear Data Tables* **1974**, *14*, 177; *J. Chem. Phys.* **1974**, *60*, 3342.

(42) Koopmans, T. C. *Physica* **1939**, *1*, 104.

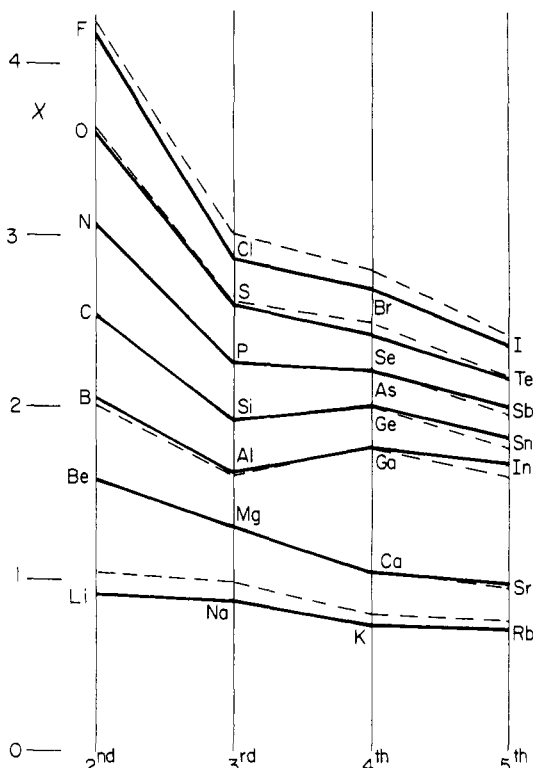


Figure 10. χ_{spec} , experimental values (solid lines), compared to Hartree-Fock-Slater χ_{HFS} (dashed lines). Data from ref 44.

method employing the Slater statistical exchange potential.⁴³ The data to construct this figure were obtained from the book by Herman & Skillman who numerically computed these wave functions, their one-electron energies, and their effective potentials for all atoms in the Periodic Table.⁴⁴ Coulomb and exchange effective potentials were also averaged over angles thereby yielding multiplet-averaged solutions, and it is obvious from Figure 10 that for our purposes these approximations are very good indeed. The Hartree-Fock-Slater scheme is computationally simpler than the straight Hartree-Fock method itself and it was originally introduced for this purpose. Subsequent research^{45,46} has showed that the statistical exchange approximation employed partially compensates antiparallel spin pair correlation effects, thereby producing good estimates for experimental one-electron energies—just the ingredients we need for constructing χ_{spec} . Thus, the good agreement between experimental χ_{spec} and χ_{HFS} computed from Herman & Skillman's tabulation of the Hartree-Fock-Slater one-electron energies provides an independent test of χ_{spec} values (Table III).⁴⁷ It is also the justification for use of Herman &

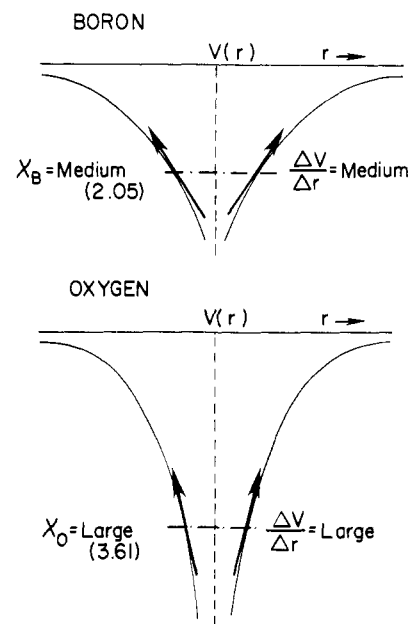


Figure 11. Schematic of effective radial potentials showing χ_{spec} and force $= -\Delta V/\Delta r$ for boron and oxygen. The diagram illustrates the qualitative correlation between χ_{spec} and the force at an atomic radius.

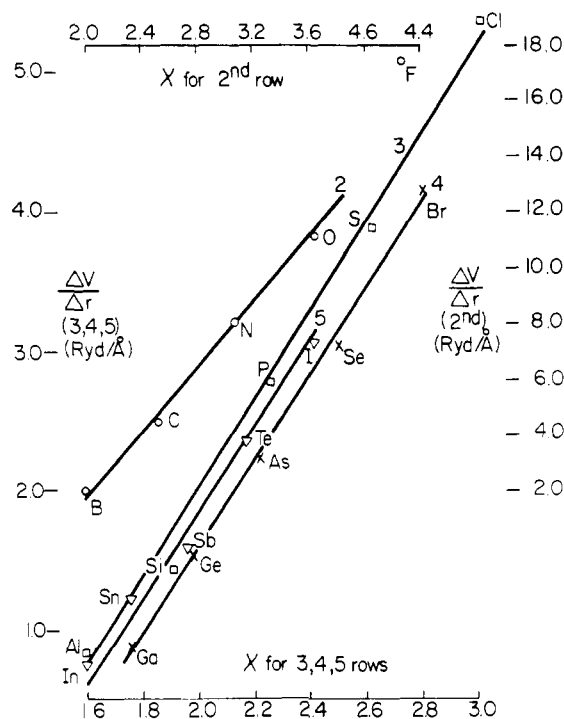


Figure 12. Relationship between χ_{spec} (Pauling units) and force $(-\Delta V/\Delta r, \text{Ry}/\text{\AA})$ at atomic radii equal to the outer radial maxima of the valence orbitals (\AA). Data from ref 44.

Skillman's tabulated effective potentials to determine the relationship between χ_{spec} and force described below.

VI. Relationship between χ_{spec} and Force at an Atomic Radius

As noted previously, the practical utility, ease of obtaining values for all atoms, and the heuristic appeal of a force definition have made the Allred & Rochow scale⁷ an important reference point in all discussions of electronegativity. Because of the intrinsic properties of funnel-shaped effective potentials it is easy to make a qualitative connection between χ_{spec} and force $= -\Delta V/\Delta r$, as shown in the Figure 11 schematic. For typical atoms, B with a medium value of χ_{spec} , and O with a large value of χ_{spec} , it is clear

(43) Slater, J. C. *Phys. Rev.* **1951**, *81*, 385.

(44) Herman, F.; Skillman, S. *Atomic Structure Calculations*; Prentice-Hall: New York, 1963. The Hartree-Fock-Slater scheme employed in these calculations is only defined for two or more electrons and therefore no value for the hydrogen atom is obtained.

(45) Slater, J. C. *Phys. Rev.* **1968**, *165*, 658. The remarkable agreement between experiment and Hartree-Fock-Slater one-electron energies for atoms throughout the Periodic Table was already known to Herman and Skillman and is impressively demonstrated by Figures 5 and 6 in their book.⁴⁴

(46) McNaughton, D. J.; Smith, V. H. *Int. J. Quantum Chem.* **1970**, *IIIS*, 775.

(47) We have ignored relativistic effects because none of the calculations we have used for comparison, ref 7, 8, 41, and 44, have employed relativistic wave functions. However, we can estimate the relativistic mass-velocity and Darwin corrections for representative atoms by perturbation theory using the methods and numerical results given by Herman and Skillman⁴⁴ (energies in Rydbergs):

χ_{spec}	O	S	Se	Te	Po
nonrelativistic	1.4086	1.0141	0.9661	0.8417	0.8002
relativistic	1.4118	1.0230	1.0084	0.9313	1.0341
percent error	0.22	0.86	4.19	9.63	22.6

Thus the relativistic correction is less than 10% for the atoms we have considered, but it is quite large for the sixth row.

Table IV. Relationship between χ_{spec} and Force at the Outer Radial Maximum^a

atom	r_M^b	$\Delta V/\Delta r^c$	χ_{spec}^d
Li	1.631	0.212	1.047
Be	1.009	1.022	1.558
B	0.762	1.976	2.020
C	0.634	4.548	2.527
N	0.524	8.111	3.072
O	0.464	11.373	3.651
F	0.410	17.423	4.266
Ne	0.354	25.536	4.912
Na	1.732	0.188	0.979
Mg	1.289	0.611	1.309
Al	1.255	0.845	1.596
Si	1.100	1.453	1.915
P	0.893	2.805	2.260
S	0.814	3.889	2.628
Cl	0.740	5.379	3.021
Ar	0.669	7.489	3.436
K	2.174	0.114	0.800
Ca	1.750	0.371	1.033
Ga	1.321	0.847	1.760
Ge	1.119	1.540	1.977
As	1.014	2.242	2.228
Se	0.911	3.039	2.504
Br	0.857	4.147	2.799
Kr	0.803	5.280	3.111
Rb	2.326	0.104	0.753
Sr	1.948	0.314	0.954
In	1.462	0.764	1.586
Sn	1.290	1.244	1.758
Sb	1.200	1.597	1.960
Te	1.112	2.269	2.182
I	1.025	3.094	2.418
Xe	1.019	3.283	2.664

^aAll data from Herman and Skillman, *Atomic Structure Calculations*, ref 44. ^b r_M in Å. ^c $\Delta V/\Delta r$ in Ry/Å. ^dPauling units. χ_{spec} average of Ge and As matched to combined average of Allred and Rochow and Pauling Ge and As, thus absolute values in Rydbergs are multiplied by 2.59184.

that the slope, $\Delta V/\Delta r$, at an r value near to where χ_{spec} crosses the potential curve has a medium magnitude for B and a large magnitude for O. Beyond this qualitative relation we must be more specific as to the definition of the radius. Allred & Rochow use the Pauling covalent radii⁴⁸ which are based on self-consistent division of experimentally determined internuclear separations for many covalently bound molecules and solids. For the quantum-mechanical wave functions and effective potentials from which we compute $\Delta V/\Delta r$, the most physically reasonable and generally employed radius is the outermost radial maximum of the atomic orbitals. The crossing point between χ_{spec} and the effective potential schematics of Figure 11, however, represents the classical turning point and corresponds to very high quantum numbers. Our ground-state orbitals therefore have outer radial maximum significantly smaller than these crossing points.

The graphs relating force and χ_{spec} shown in Figure 12 for p-block elements were calculated numerically by interpolating and differencing in the Herman & Skillman atomic wave function and effective potential tables described above (values given in Table IV). The interesting and significant feature of these graphs is the almost linear relationship between force and χ_{spec} for each p-block row and that the lines for the 3rd, 4th, and 5th rows are close together.⁴⁹ These numerical facts plus the qualitative relationship expressed by the schematic of Figure 11 enrich the conceptual and intuitive chemical utility of electronegativity.⁵⁰

(48) Pauling, L. J. *Am. Chem. Soc.* **1947**, *69*, 542.

(49) The lines for the s-block elements of groups I and II show the same relationship to one another as those of the p-block (Figure 12), but the s-block lines have a smaller slope than those of the p-block. Therefore there is no continuous single linear relationship between χ_{spec} and any row.

It should be noted, however, that there is no basic quantum-mechanical theorem that requires a linear relationship between average one-electron energies and forces at outer radial maxima for a given row in a given block and none implying that a single formula, like that of Allred & Rochow, should be able to fit all of the representative elements.⁵¹

VII. Bond Polarity Index²⁸

A paper of this title is to be submitted soon,²⁸ and we give here only the resulting quantum-mechanical formulae and definitions that bear on $\Delta\chi_{\text{spec}}$ and a single specific example. We employ a single determinant molecular orbital wave function (it is readily generalized to a configuration interaction wave function) and assume an LCAO expansion, $\psi_i = \sum C_{ki}\phi_k$, and that ψ_i satisfies the Roothaan equations in canonical form. The index i designates the N MOs, n_i their occupancy, and ϵ_i their one-electron energies. The indices j, k designate the M AOs in the basis set. We are interested in the average energy of atom A, with $M(A)$ AOs, in a molecule or solid with M AOs. The projection of ϕ_j on MO i is $\int C_{ji}\phi_j\psi_i d\tau$ and the energy of this AO in the molecule is the sum over all MOs of $n_i\epsilon_i \int C_{ji}\phi_j\psi_i d\tau$. If this quantity, in turn, is summed over the AOs of atom A we get the in situ energy of atom A. The average energy (per electron) of this atom, called the energy index, EI_A , is then given by the formula

$$EI_A = \sum_i n_i \epsilon_i \sum_j \sum_k^{M(A)} C_{ji} C_{ki} S_{jk} / \sum_i n_i \sum_j \sum_k^{M(A)} C_{ji} C_{ki} S_{jk}$$

where S_{jk} is the atomic orbital overlap integral, $\int \phi_j \phi_k d\tau$.⁵² The Bond Polarity Index represents in situ $\Delta\chi_{\text{spec}}$ and the covalent bonding component must be subtracted out, thus

$$BPI_{AB} = (EI_A - EI_A^{\text{ref}}) - (EI_B - EI_B^{\text{ref}})$$

where EI_A^{ref} is EI_A for the corresponding homonuclear bond AA and subtracts out its pure covalent energy component. For example, for the C-F bond in $\text{H}_3\text{C-F}$ we compute EI_C and EI_F , but also EI_C^{ref} in $\text{H}_3\text{C-CH}_3$ and EI_F^{ref} in F-F . With use of the 6-31G* basis set and atomic units, $EI_C = -0.743$, $EI_F = -0.881$, $EI_C^{\text{ref}} = -0.665$, $EI_F^{\text{ref}} = -0.983$, and $BPI_{CF} = -0.180$ au.²⁸ We can convert these into a *Fractional Polarity* by dividing BPI_{AB} by the energy required to take an electron from A to B, and this number is the energy equivalent of Pauling's dipole moment determined percent ionic character.¹⁰ For the $\text{H}_3\text{C-F}$ example ($r_{CF} = 1.383$ Å) the fractional polarity is 47%.

(50) This qualitative association is enhanced by the work of Boyd and Markus (*J. Chem. Phys.* (1981) **77**, 5385), who employed a special set of large-valued radii (e.g., C, 1.54 Å; N, 1.36; O, 1.27) and assumed $\chi_A \approx Z_A/r_A^2(1 - \int \phi^2 D(r) dr)$ where the radial charge density $D(r)$ is obtained from the Clementi and Roetti Hartree-Fock atomic orbitals. Their χ_A show the same general pattern as the Mulliken definition values of Figure 6 (but groups II and III do not overlap), and perhaps this is not surprising because as $r \rightarrow \infty$ the charge density is known to fall off as $\exp(-I_A r)$. Unfortunately, use of smaller values of r_A , such as those used by Allred and Rochow or the outer radial maxima, do not lead to useful χ (R. J. Boyd, private communication). This appears to be the result of assuming the force to be inversely proportional to a radius squared thus imposing the concept of a classical radius onto a quantum mechanical charge distribution.

(51) The fact that the Allred and Rochow formula fits the 2nd row values without re-referencing as would be suggested by the considerably different slope and range of $\Delta V/\Delta r$ versus χ_{spec} for this row compared to the 3rd, 4th, and 5th appears to result from a fortuitous choice of covalent radii. Allred and Rochow chose the larger of the two sets of radii offered by Pauling in his 1947 tabulation⁴⁸ while the radial maxima parallel the smaller set and, in fact, are significantly smaller still.

(52) EI_A gives insight into the atomic binding process and the dependence of electronegativity on oxidation state. When one representative element binds to another the average valence shell energy of the atom with lower electronegativity will move to lower energy and vice versa, i.e. the transfer of charge during binding leads to a compacting of atomic energy levels but does not alter the identity of the atoms. For example, free atom EI_A at 6-31G* compared to EI_A in AH_2 (in parenthesis, atomic units) are as follows: F, -0.953 (FH, -0.892); O, -0.823 (OH, -0.772); N, -0.720 (NH, -0.694); C, -0.567 (CH, -0.661); B, -0.426 (BH, -0.568); Be, -0.302 (BeH, -0.465); Li, -0.196 (LiH, -0.300). The energy level compacting is in the direction expected and the change in oxidation states does not change the ordering of the electronegativities thereby rationalizing the observation of representative element chemists that dependence of electronegativity on oxidation state is generally not required.

Group or Substituent Electronegativity. This is defined as the difference in electronegativity across a bond AB where A is a reference atom (or molecular fragment) and B is the group of interest (e.g., $-\text{CH}_3$, $-\text{CHO}$, $-\text{CCH}_3$, $-\text{CHCH}_2$, $-\text{CH}_2\text{CH}_3$, $-\text{CH}_2\text{OH}$, $-\text{CO}_2\text{H}$, $-\text{NH}_2$, $-\text{OCH}_3$, $-\text{SiH}_3$, etc.). There are several excellent, up-to-date reviews of this important physical organic chemistry topic^{53,54} and it is apparent that there is considerably less agreement on values for the 25–35 most studied groups than there is for the approximately equal number of individual atoms (Allred & Rochow and Pauling scales). Calculation of group electronegativities is a direct application of the Bond Polarity Index, BPI_{AB} , and results to-date appear promising.²⁸ A principal point for our purpose here is the possibility of making close connection between the success achieved by χ_{spec} in reproducing the Allred & Rochow and Pauling scales and the expectation that its in situ translation into BPI_{AB} can similarly provide the basis for accurate and well-defined values for this physically and synthetically useful quantity.

Electronegativity Perturbations on Molecular Orbital Energy Level Diagrams. Much of the conceptual understanding of organic and inorganic chemistry during the last quarter century has been achieved through the use of qualitative and semiquantitative molecular orbital theory, and the effect of electronegativity perturbations on molecular orbital energy levels has been a prominent theme.^{55–59} Are the assumptions concerning the nature and definition of electronegativity throughout this development compatible with those we have put forward here? The formula given for EI_A above demonstrates an affirmative answer and we also show that the new definition can lead to an extension and refinement of the existing qualitative and semiquantitative treatments.

In the majority of applications a single type of AO is used (typically a $2p\pi$) and an increase in electronegativity of a specified atom has been modeled by lowering the atomic Coulomb integral for that atom. Changes in the MOs are then determined by first- and second-order perturbation theory.⁵⁵ With only one type of AO, average and individual orbital energies are identical, and when the same approximations with respect to overlaps are made in the EI_A expression and in the perturbation theory, the resultant electronegativity perturbations of the MOs will be the same and thus within the conceptual framework put forth in this paper. Starting with single AO homonuclear reference systems, Albright, Burdett, and Whangbo give three illuminating examples⁵⁵ (π orbitals for $\text{A}_2 \rightarrow \text{AB}$ and benzene \rightarrow pyridine, $\text{H}_2 \rightarrow \text{HH}'\text{H}$, and HHH') and show how electronegativity perturbation results from these simple, special cases have wide ramifications in the qualitative understanding of substituent effects in organic structure and reactivity. In the examples noted here the actual magnitude of the electronegativity perturbation is left unassigned as only qualitative trends were desired, but if needed, its magnitude could be determined directly by the EI_A formula.

For many representative element inorganic systems (e.g., AB_4 , AB_5 , AB_6) Gimarc has constructed qualitative molecular orbital energy level diagrams and invoked electronegativity perturbations to successfully rationalize trends in their geometrical and spectroscopic properties.⁵⁶ Both s and p AOs are required to construct

suitable MOs for these molecules and a useful example is tetrahedral AB_4 subject to a perturbation that significantly lowers the electronegativity of A (e.g., Cl_4 to SnI_4). When A lowers its electronegativity two changes occur in its orbitals: their center of gravity moves to higher energy and the s–p separation gets smaller. In T_d AB_4 for 8 valence electrons the LUMO and LUMO+1 levels are $2a_1$, $2t_1$ and $2t_1$, $2a_1$, respectively,⁵⁶ the reversal largely brought about by the reduction in s–p separation. When molecular orbitals are constructed directly from the free atom AOs their relationship to electronegativity is just χ_{spec} , but when MOs are to be made out of the orbitals of molecular fragments and an atomic or group electronegativity perturbation then invoked, the most straightforward approach is to construct the MOs for the systems with and without perturbation and then calculate BPI_{AB} to determine, a posteriori, the electronegativity difference caused by the perturbation.

Electronegativity of Hybridized Orbitals. In part II of this paper we have noted that the Mulliken-derived concept of hybrid orbital electronegativity suffers from a general inability to make a priori hybridization assignments, yet for certain cases the ordering of electronegativity magnitudes according to hybridization is so common in organic chemistry⁶⁰ that it should be reflected in χ_{spec} and EI_A . The most important example is the σ orbital ordering rule (highest to lowest electronegativity) $\text{sp} > \text{sp}^2 > \text{sp}^3$. The qualitative truth of this ordering is as apparent in free atom χ_{spec} or in EI_A as it is in any of the electronegativity definitions that have been specifically formulated in terms of hybrid orbitals: the greater the percent s character the larger the value of χ_{spec} simply because s electrons have a lower energy than p electrons.⁶¹

Electronegativity and Atomic Charge. The definition of χ_{spec} as a free atom property precludes any direct relationship with in situ atomic charge just as the Periodic Table is unable to characterize details of the bonding between atoms. On the other hand, chemists have always assumed the existence of a strong correlation between χ and in situ atomic charge. This belief is fully justified by computational results using the in situ index BPI_{AB} .²⁸ However, in making the connection with BPI_{AB} , the long-standing and incompletely resolved problems with quantum-mechanical charge definitions themselves need to be addressed.⁶² Thus, it is significant that in almost all chemical applications it is *bond polarity*, not atomic charge, that is the property of ultimate concern, and it may turn out that atomic charge will be much less needed in the future. In addition, since BPI_{AB} is an energy, it follows from perturbation theory that it is determined to higher order than the charge, and therefore less sensitive to basis set changes than most quantum-mechanical charge definitions.⁶³

VIII. Experimental Measurement of $\chi_{\text{spec}}^\text{A}$ and EI_A

Everyone recognizes that even though the properties of free atoms are governed by the laws of physics and therefore directly obtainable from physical measurements, their particular array in rows and columns which constitutes the Periodic Table is not

(53) *Prog. Phys. Org. Chem.*; Taft, R. W., Ed.; Wiley-Interscience: New York, 1987; Vol. 16. See particularly: Taft, R. W.; Topsom, R. D. The Nature and Analysis of Substituent Electronic Effects and Topsom, R. D. Some Theoretical Studies of Electronic Substituent Effects in Organic Chemistry.

(54) Isaacs, N. S. *Physical Organic Chemistry*; Longmans Science & Technology, 1987.

(55) Albright, T. A.; Burdett, J. K.; Whangbo, M.-H. *Orbital Interactions in Chemistry*; Wiley-Interscience: New York, 1985; Chapter 6, pp 80–86.

(56) Gimarc, B. M. *Molecular Structure and Bonding, The Qualitative Molecular Orbital Approach*; Academic Press: New York, 1979; Chapters 1, 3, 4, 5, and 7. For the AB_4 case see pp 62 and 63 and: Gimarc, B. M.; Khan, S. A. *J. Am. Chem. Soc.* **1978**, *100*, 2340.

(57) Fleming, I. *Frontier Orbitals and Organic Chemical Reactions*; Wiley-Interscience: New York, 1976; Chapters 2, 3, and 4.

(58) Jorgensen, W. L.; Salem, L. *The Organic Chemist's Book of Orbitals*; Academic Press: New York, 1973; Chapter 1.20.

(59) Streitwieser, A., Jr. *Molecular Orbital Theory for Organic Chemists*; Wiley: New York, 1961; Chapter 5.

(60) Lowry, T. H.; Richardson, K. S. *Mechanism and Theory in Organic Chemistry*, 3rd ed.; Harper & Row: New York, 1987; Carey, F. A. *Organic Chemistry*; McGraw-Hill: New York, 1987; Ternay, A. L., Jr. *Contemporary Organic Chemistry*, 2nd ed.; W. B. Saunders, 1979; March, J. *Advanced Organic Chemistry*; McGraw-Hill: New York, 1977.

(61) The set of molecules usually given to illustrate this ordering rule is $\text{HC}\equiv\text{CH}$, $\text{H}_2\text{C}=\text{CH}_2$, and $\text{H}_3\text{C}-\text{CH}_3$, and it is certainly true that the acidity of the σ orbital bound hydrogens follows the order given. But it is not necessary that an in situ electronegativity for the carbon atom itself follows this same order because of the difference in multiple bonding for the three cases (in fact, EI_C for these molecules shows the opposite order).

(62) A quite different way of relating atomic charge to electronegativity, and one that is as compatible as possible with free atom electronegativities, is the Lewis–Langmuir definition applicable to Lewis Dot structures. For atom A in bond AB this scheme uses the ratio $\chi_\text{A}/(\chi_\text{A} + \chi_\text{B})$ to interpolate between formal charge (covalent extreme) and oxidation number (ionic extreme) (Allen, L. C. *J. Am. Chem. Soc.*, in press).

(63) Since BPI_{AB} represents the difference in energy between an average electron in atom A and in atom B, why do all the electrons not transfer to the most electronegative atom? (1) BPI_{AB} is a one-electron energy difference and, as is well-known in Hartree–Fock theory, the sum of the one-electron energies is on the order of one-half the total energy, the rest being electron–electron repulsion (Coulomb and exchange terms). (2) The Pauli principle restricts penetration of one atom by another just as it accounts for the impenetrability of matter in general.

measurable, i.e., the Periodic Table is a *chemical pattern recognition* scheme that belongs to the set of concepts immediately above physics in the complexity hierarchy of science, often termed "broken symmetry".^{64,65} Thus the corresponding array of χ_{spec}^A (and $\Delta\chi_{\text{spec}}^{AB}$) that we have identified as the third dimension of the Periodic Table gives trends for the *chemical* property, *bond polarity*, a quantity not obtainable from direct physical measurement, even though values for individual elements (and for $\Delta\chi_{\text{spec}}^{AB}$) can be determined to high accuracy from atomic spectroscopy. The usefulness of this categorization is that it removes the frequent misconception of electronegativity as an inherently "fuzzy" quantity of somewhat questionable significance. EI_A and BPI_{AB} , chemical indices appropriate for specific molecular and solid-state environments, are similarly outside the domain of direct physical measurement.²⁸

IX. Summary

1. Electronegativity, χ_{spec} , is the average one-electron energy of valence shell electrons in ground-state free atoms and may be identified as the third or energy dimension of the Periodic Table. This definition, $\chi_{\text{spec}} = (m\epsilon_p + n\epsilon_s)/(m + n)$, where m , ϵ_p , n , and ϵ_s are the number and ionization energies of the p and s electrons of the representative elements, leads to precision values obtainable from high-resolution atomic spectroscopy.

2. The electronegativity of transition-metal elements is likewise the average valence shell energy, $(m\epsilon_d + n\epsilon_s)/(m + n)$, but it is often difficult to assign m , the number of d electrons, and this is reflected in the infrequent usage of this quantity among transition-metal chemists. A simple bonding assumption for the first transition series permits approximate estimates.

3. The variation in electronegativity (and increase in groups I–V metallization) down a column in the Periodic Table and its increase across a row, the existence of the diagonal metalloid band separating metals from non-metals, and the chemistry of the noble gas molecules can be deduced from the χ_{spec} definition.

4. The progressive changes in bonding from covalent to ionic, from the alkali metals through the metal/non-metal transition to covalent molecules, and from metallic to ionic bonds are all characterizable by changes in χ_{spec} and $\Delta\chi_{\text{spec}} \equiv \chi_{\text{spec}}^A - \chi_{\text{spec}}^B$ across bond AB. Many of the changes from one bond type to another are separated by regions where polymeric materials predominate and χ_{spec} delineates the boundaries of these regions.

5. The principal properties of other types of bonds, e.g. hydrogen bonds, A–H...B, and Alcock's secondary bonds, A–Y...B, (which occur widely in inorganic solids for $\chi_{\text{spec}}^A > \chi_{\text{spec}}^B$) are also characterizable by χ_{spec} and $\Delta\chi_{\text{spec}}$.

6. An analysis of the literature on chemical usage of electronegativity since Pauling put forth his scale in 1932 shows that only his and the force definition scale of Allred & Rochow have been repeatedly employed by practicing chemists, therefore the finding that χ_{spec} reproduces the pattern of these two established scales is of first importance. Moreover, the close match achieved enables χ_{spec} to referee differences between them, thus showing that $\chi_N > \chi_{\text{Cl}}$ and resolving the troublesome discrepancies in 5th row values. The tight fit realized between χ_{spec} and a very recent report of p-block electronegativities based on computed electronic charge distributions also support its validity. In addition to these comparisons for representative elements, estimates for first transition series χ_{spec} parallel those of Allred's Pauling scale experimental values.

7. Hartree–Fock atomic calculations of χ_{spec} are found to reproduce the principal features of the multiplet averaged experimental values. The spherically averaged and antiparallel spin-correlated χ_{spec} values obtained from Hartree–Fock–Slater calculations prove to be even closer to the experimental numbers, thereby acting as an internal check for representative element χ_{spec} and providing useful data for the transition-metal estimates.

8. The chemical bond characterizing capabilities summarized above for free atom, ground state χ_{spec} show it plus the usual two dimensional Periodic Table capable of organizing overall trends in chemical structure and reactivity, but do not themselves provide numbers for specific bonds in specific molecules or solids. To get specific numbers for particular molecules or solids it is necessary to set up the electronic wave functions for the molecule or solid in question and calculate expectation values corresponding to the average energy of an atom A or the difference in energy between an average electron in atom A and an average electron in an adjacent atom B. Formulae for these in situ atom A and bond AB expectation values have been derived and called the *Energy Index*, EI_A , and the *Bond Polarity Index*, BPI_{AB} , respectively (they are treated more fully in a forthcoming article).

9. EI_A and BPI_{AB} are chemical indices that quantify the electronegativity concepts that have been used in qualitative and semiquantitative molecular orbital theory during the last quarter century. Three areas of applications are particularly significant: (a) group (substituent) electronegativity—determination of this important and long-debated physical organic chemistry parameter can be carried out as a direct application of BPI_{AB} with A as reference atom or fragment and B as the group of interest; (b) electronegativity perturbations of molecular orbital energy level diagrams—A change in electronegativity of an atom A in the bond AB from χ_A to $\chi_{A'}$ implies a change in the average energy of the one-electron levels of A to that of A' and is measured by the change in bond polarity $\text{BPI}_{AB} \rightarrow \text{BPI}_{A'B}$; (c) electronegativity of hybrid orbitals. In most cases of interest to organic chemists, e.g., $\chi_{\text{sp}} > \chi_{\text{sp}}^2 > \chi_{\text{sp}}^3$, the ordering rules can be deduced immediately from the definition of free atom χ_{spec} without elaborate formulation or calculation. In general, the electronegativity of specific hybrids in specific molecular environments can be computed by BPI_{AB} .

Note Added in Proof. We inadvertently omitted helium in our figures and tables. χ_{spec} for He from the NBS Tables¹ is 1.8074 Rydbergs $\cong 4.2$ in Pauling units (scale factor in Table I). χ_{spec} for F is also $\cong 4.2$ and Ne at $\cong 4.9$ is the highest value in the Periodic Table. These values predict that HeF_2 will not be bound and this conclusion is verified by results from extensively correlated ab initio valence bond wave functions (Allen, L. C.; Erdahl, R. M.; Whitten, J. L. *J. Am. Chem. Soc.* **1965**, *87*, 3769. Allen, L. C.; Lesk, A. M.; Erdahl, R. M. *Ibid.* **1966**, *88*, 615). The latter reference also includes the repulsive potential energy curve for the linear symmetric stretch of NeF_2 and this curve rises much more steeply than that for HeF_2 in accordance with the size and χ_{spec} of Ne compared to He. It may also be recalled that the textbook repulsive interaction example of HeH shows a relatively flat repulsive curve both theoretically and experimentally (Taylor, H. S.; Harris, F. E. *Mol. Phys.* **1963**, *7*, 287).

Acknowledgment. The author thanks his graduate students, Eugene T. Knight and Congxin Liang, for the many stimulating discussions, suggestions, and critical comments that have greatly aided this research. He also acknowledges the numerous useful suggestions given by Professor Joel F. Liebman and an anonymous referee.

(64) Anderson, P. W. *Science* **1972**, *177*, 393.

(65) Primas, H. *Chemistry, Quantum Mechanics and Reductionism*; Springer-Verlag: New York, 1983.